

000 001 002 003 004 005 006 007 008 009 010 011 012 013 014 015 016 017 018 019 020 021 022 023 024 025 026 027 028 029 030 031 032 033 034 035 036 037 038 039 040 041 042 043 044 045 046 047 048 049 050 051 052 053 PACR: PROGRESSIVELY ASCENDING CONFIDENCE RE- WARD FOR LLM REASONING

Anonymous authors

Paper under double-blind review

ABSTRACT

Reinforcement Learning with Verifiable Rewards (RLVR) has significantly improved LLM reasoning, but its sparse, outcome-based reward provides no guidance for intermediate steps, slowing exploration. We propose Progressively Ascending Confidence Reward (PACR), a dense, model-intrinsic reward computed directly from the model’s evolving belief in the correct answer. PACR encodes the inductive bias that, along a well-formed reasoning trajectory, the probability of the ground-truth answer should have a generally ascending trend. We provide empirical and theoretical analysis validating that such an inductive bias constrains the exploration search space to regions richer in logically sound reasoning. We demonstrate that PACR accelerates exploration, reaches reward saturation with fewer trajectories, and yields improvements on multiple benchmarks. Our results suggest that dense, model-intrinsic shaping signals can make RLVR training more effective and reliable. Code will be released.

1 INTRODUCTION

Pre-trained large language models (LLMs) exhibit strong performance on complex, multi-step reasoning tasks (Comanici et al., 2025; Yang et al., 2025a; Team, 2025). Reinforcement Learning with Verifiable Rewards (RLVR) has emerged as a leading approach for further improving such capabilities, using a programmatically checkable terminal metric (e.g., exact-match on the final answer) as the reward (Shao et al., 2024b; Guo et al., 2025). While effective, the standard RLVR formulation supplies a sparse terminal accuracy signal, offering no guidance for intermediate steps and thus exacerbating credit assignment. Alternative process-based supervision employs external reward models to score intermediate reasoning, but is costly to train, data-hungry, and prone to misalignment (Cui et al., 2025; Cheng et al., 2025).

This work asks whether we can obtain *stepwise supervision* directly from the model. Psycholinguistic work shows that people interpret language incrementally, updating expectations with each word; as context accumulates, uncertainty falls and the correct interpretation becomes more likely (Hale, 2001; Levy, 2008). By the same logic, in tasks with a verifiable final answer, a correct intermediate step should typically raise the model’s probability of the ground-truth answer. Concretely, given a question q , a reasoning prefix $H_{\leq k}$, and ground truth Y_{gt} , we track the model’s confidence $p(Y_{\text{gt}} | q, H_{\leq k})$ and expect a general upward trend over steps (Figure 1).

Guided by this premise, we introduce the **Progressively Ascending Confidence Reward (PACR)**, a dense, model-intrinsic signal that converts confidence growth into stepwise supervision for LLM reasoning during reinforcement learning. During training, as the model produces a sequence of reasoning steps for a question with a verifiable answer, we evaluate at each step the log-probability assigned to the ground-truth answer and reward any positive change, effectively encouraging a consis-

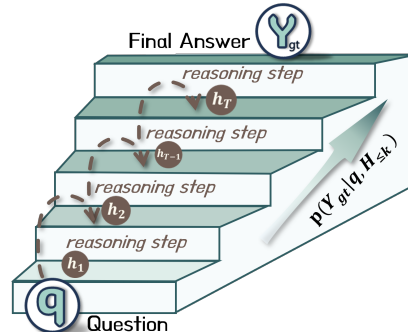


Figure 1: **Stepwise confidence growth.** For a question q , a well-formed sequence of reasoning steps h_1, \dots, h_k should increase the model’s probability of the ground-truth answer Y_{gt} across steps.

tently upward trend in confidence. Because PACR is computed from the model’s own probabilities, it requires no external reward model and is available at every step, improving credit assignment and steering search toward faithful trajectories. We pair PACR with the standard RLVR terminal accuracy reward so the objective remains anchored to verifiable correctness while the process signal shapes the reasoning path. **In detail, our contributions can be summarized as follows:**

- **Empirical Validation of an Inductive Bias (Section 4.1).** We provide extensive observational evidence that ground-truth confidence growth acts as a powerful inductive bias. Our analyses on open-source LLMs reveal three key findings: (1) a *consistent* confidence ascent strongly correlates with final answer correctness; (2) among correct answers, logically coherent reasoning paths exhibit an even *more consistent* ascent than spurious ones; and (3) the *magnitude* of the confidence gain effectively pinpoints pivotal reasoning steps.
- **Theoretical Justification (Section E and 5).** We provide a theoretical foundation for using confidence growth as a process reward. We prove that a reasoning step from an idealized oracle policy will, on average, increase or maintain the model’s confidence in the ground truth, validating it as a strong inductive bias. Building on this, we formalize the **Progressively Ascending Confidence Reward (PACR)** and introduce two concrete methods for its implementation: **Sparse-PACR** for trajectory-level rewards and **Dense-PACR** for step-wise rewards.
- **Experimental Results (Section 7).** Across multiple reasoning benchmarks, augmenting RLVR with our PACR methods improves training dynamics and final performance. Our approach accelerates exploration and ultimately attains a higher, more consistent final score than the baseline, demonstrating a more effective and reliable training process.

2 RELATED WORK

Outcome-based RL for LLM Reasoning Reinforcement Learning (RL) is increasingly used to fine-tune Large Language Models (LLMs). This is done not only to align models with human preferences via Reinforcement Learning from Human Feedback (RLHF) (Ouyang et al., 2022; Li et al., 2024b; Bai et al., 2022) but also to enhance their reasoning abilities for complex problem-solving (Kumar et al.). To improve these reasoning capabilities, a recent prominent approach is Reinforcement Learning with Verifiable Reward (RLVR) (Guo et al., 2025; Yang et al., 2024; Shao et al., 2024a), which uses an outcome-based reward instead of a proxy reward model. For example, a reward of 1 is assigned for a correct answer and 0 (or -1) for an incorrect one. Then, the model generates multiple trajectories for a single problem. The reward for each trajectory is then compared against the average reward across all samples in the group, and this relative reward is used as an advantage to train the model. This outcome-based reward system is widely explored (Liu et al., 2025b; Yu et al., 2025; Hu et al., 2025; Zeng et al., 2025b) because it is easily scalable, and mitigates concerns about reward hacking by eliminating the need for a separate reward model (Guo et al., 2025). However, this approach has a significant limitation for complex reasoning tasks that require generating a long thought process (Zhang et al., 2025). In such cases, relying solely on the final outcome provides a sparse and noisy reward signal.

Dense Reward for LLMs Finetuning with RL To overcome the limitations of holistic, trajectory-level sparse rewards, various approaches for providing dense rewards have been explored. In RLHF, for instance, approaches include training an external reward model to assign token-level rewards using synthesized data (Yoon et al., 2024), utilizing a more mature external model as the reward model (Cao et al., 2024; Wu et al., 2023), and use implicit reward signal from reward model (Chan et al., 2024). Similarly, direct alignment algorithms (e.g., DPO (Rafailov et al., 2023)) have been adapted to provide dense rewards by re-framing DPO’s implicit reward at a token level (Zeng et al.; Zhu et al.; Zhong et al.; Rafailov et al.) or by selectively using specific tokens for the reward signal (Yoon et al.; Liu et al.). For training a reasoning LLM with RL, previous approaches include training a Process Reward Model (PRM) for process-level rewards (Li & Li, 2025; Cheng et al., 2025; Zhang et al., 2025), or defining a DPO-like implicit reward at the token level (Cui et al., 2025; Yuan et al., 2024). However, these approaches typically require additional models, such as a reward model or a reference model, to generate the reward signal. In contrast, our work eliminates the need for any additional models. We instead use the current policy model itself to generate a dense reward signal that enhances reasoning capabilities.

108

3 BACKGROUND AND PROBLEM SETUP

109

110 This section introduces the notation for reasoning trajectories, how we segment and evaluate stepwise
111 confidence in the ground-truth answer, and the RL objective we use in training.
112

113 **Reasoning Trajectories and Notation.** Given a question q , a policy π_θ generates a *sequence of*
114 *reasoning steps* $H = (h_1, \dots, h_T)$ and a final answer \hat{Y} . Let Y_{gt} denote the verifiable ground-truth
115 answer. We write $H_{\leq k} = (h_1, \dots, h_k)$ for the reasoning steps up to step k . We analyze and shape
116 the reasoning process by tracking how the model’s probability of Y_{gt} evolves with the prefix $H_{\leq k}$.
117

118 **Segmenting the Reasoning Process and Stepwise Ground-truth Confidence.** Similar to Yang
119 et al. (2025c), we segment each generated reasoning trace into discrete steps $\{h_k\}_{k=1}^T$ using a simple,
120 model-agnostic rule: start a new step at a newline (‘\n’) or at a period followed by a space (‘. ’);
121 fragments shorter than five tokens are merged with the preceding step to avoid overly fine splits
122 ([Further discussion on segmentation strategies is provided in Appendix B](#)). To measure ground-
123 truth-anchored confidence at step k , we standardize the answer format by appending a short prefix
124 y_{gt}^0 (e.g., ‘So the final answer is \boxed{’) and evaluate the model’s probability of the
125 ground-truth answer $Y_{\text{gt}} = (y_{\text{gt}}^1, \dots, y_{\text{gt}}^L)$ under the current prefix $H_{\leq k}$. Writing $Y_{\text{gt}} = (y_{\text{gt}}^1, \dots, y_{\text{gt}}^L)$,
126 we measure the **ground-truth confidence** at step k as
127

$$\log p(Y_{\text{gt}}|q, H_{\leq k}) = \sum_{l=1}^L \log p_\theta(y_{\text{gt}}^l | q, H_{\leq k}, y_{\text{gt}}^0, y_{\text{gt}}^{<l}), \quad (1)$$

130 where $y_{\text{gt}}^{<l}$ are preceding answer tokens. This measures the model’s confidence in the ground truth
131 answer at any given stage of its reasoning steps.
132

133 **Group Relative Policy Optimization (GRPO)** GRPO (Shao et al., 2024b) estimates advantages
134 by comparing returns *within* a group of N samples rather than using a learned value function. For a
135 given question q (with verifiable answer Y_{gt}), the behavior policy $\pi_{\theta_{\text{old}}}$ generates N trajectories
136

$$\{\tau^{(i)}\}_{i=1}^N, \quad \tau^{(i)} = (H^{(i)}, \hat{Y}^{(i)}), \quad (2)$$

138 where $H^{(i)} = (h_1^{(i)}, \dots, h_{T_i}^{(i)})$ are the reasoning steps, T_i is the number of steps for i -th trajectory
139 and $\hat{Y}^{(i)}$ is the predicted answer for i -th trajectory.
140

141 For each sampled trajectory i , we compare the predicted answer $\hat{Y}^{(i)}$ with the ground truth Y_{gt} and
142 assign a binary terminal accuracy reward:
143

$$R^{(i)} = \begin{cases} 1, & \text{is_equivalent}(\hat{Y}^{(i)}, Y_{\text{gt}}) \\ 0, & \text{otherwise.} \end{cases} \quad (3)$$

146 Here `is_equivalent` performs task-specific normalization (e.g., stripping whitespace/punctuation,
147 handling LaTeX boxing, case folding, and numeric tolerances) before exact match. The group-relative
148 advantage for trajectory i is computed by centering (and optionally standardizing) its reward within
149 the cohort of N samples:
150

$$A^{(i)} = \frac{R^{(i)} - \text{mean}(\{R^{(i)}\}_{i=1}^N)}{\text{std}(\{R^{(i)}\}_{i=1}^N)}. \quad (4)$$

153 Similar to PPO (Schulman et al., 2017), GRPO adopts a clipping with KL penalty:
154

$$\mathcal{J}_{\text{GRPO}}(\theta) = \mathbb{E}_{\substack{(q, Y_{\text{gt}}) \sim \mathcal{D} \\ \{\tau^{(i)}\} \sim \pi_{\theta_{\text{old}}}(\cdot|q)}} \left[\frac{1}{N} \sum_{i=1}^N \frac{1}{|\tau^{(i)}|} \left(\min \left(\frac{\pi_\theta(\tau^{(i)} | q)}{\pi_{\theta_{\text{old}}}(\tau^{(i)} | q)}(\theta) A^{(i)}, \text{clip} \left(\frac{\pi_\theta(\tau^{(i)} | q)}{\pi_{\theta_{\text{old}}}(\tau^{(i)} | q)}, 1 - \varepsilon, 1 + \varepsilon \right) A_i \right) - \beta D_{\text{KL}}(\pi_\theta || \pi_{\text{ref}}) \right) \right], \quad (5)$$

159 where \mathcal{D} is the training dataset and π_{ref} is a reference policy. In our work, we follow the Dr. GRPO
160 (Liu et al., 2025b) formulation, a bias-mitigated variant of GRPO. This approach modifies the standard
161 GRPO algorithm by discarding the standard deviation from the advantage calculation and the length
normalization from the loss function (the terms shown in **green** in Eq. 4 and Eq. 5).
162

162 4 IS GROUND-TRUTH CONFIDENCE GROWTH A USEFUL INDUCTIVE BIAS?

164 We posit that reasoning fundamentally functions as a process of *uncertainty reduction*. A faithful
 165 reasoning step provides intermediate evidence that bridges the gap to the solution, mathematically
 166 manifesting as an increase in the probability of the ground-truth answer. This suggests the following
 167 inductive bias for learning: valid reasoning steps should be characterized by **positive confidence**
 168 **gain on the ground-truth answer**.

169 To validate this inductive bias as a reward, we test two key conditions:

170

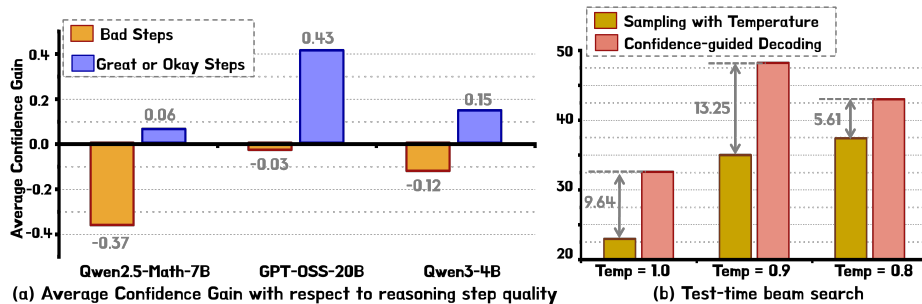
- 171 a) **Granular Quality:** Does the ground-truth confidence gain correlate with step-level reasoning
 172 quality?
- 173 b) **Causal Utility:** Does guiding generation with this bias improve accuracy during inference?

174 **Ground-truth Confidence Growth.** We first quantify confidence growth by defining the stepwise
 175 confidence gain, C_k , as the change in the log-probability of the ground-truth answer induced by the
 176 addition of reasoning step h_k :

$$178 \quad C_k := \log \pi_\theta(Y_{\text{gt}} | q, H_{\leq k}) - \log \pi_\theta(Y_{\text{gt}} | q, H_{<k}), \quad (6)$$

179 where $H_{\leq k} = (h_1, \dots, h_k)$ and $H_{<k} = (h_1, \dots, h_{k-1})$. For $k = 1$, $H_{<1}$ is the empty prefix.
 180 Intuitively, C_k measures the information gain regarding the ground truth provided by step h_k . (When
 181 indexing trajectories, we write $C_k^{(i)}$.) For brevity, we will hereafter use “confidence growth” and
 182 “ground-truth confidence growth” interchangeably.

184 4.1 OBSERVING GROUND-TRUTH CONFIDENCE GROWTH ON REASONING MODELS



196 Figure 2: **Validation of Confidence Growth Utility.** (a) **Granular Quality:** We utilized GPT-5.1
 197 to annotate individual reasoning steps as `GREAT`, `OKAY`, or `BAD`. We then analyzed the model’s
 198 **intrinsic** confidence gain (C_k) for each category. The results show that high-quality steps consistently
 199 drive positive C_k , while flawed steps yield negligible or negative gains. (b) **Causal Utility:** Using C_k
 200 to guide generation (via beam search with width 1) on Qwen2.5-Math-7B significantly improves
 201 accuracy compared to standard sampling across multiple temperatures. This confirms that maximizing
 202 confidence growth actively steers the model toward correct solutions.

203
 204 **a) Granular Quality: Does the ground-truth confidence gain correlate with step-level reasoning**
 205 **quality?** To demonstrate that C_k effectively captures reasoning quality of a step, we performed a
 206 fine-grained analysis using trajectories sampled from diverse models. We utilized an external verifier
 207 to annotate individual reasoning steps, classifying each into one of three categories based on the
 208 definitions established by Lightman et al. (2023) (refer to Appendix F for full annotation details):

209

- 210 • `GREAT`: A strong, logically sound step that makes meaningful mathematical progress.
- 211 • `OKAY`: A valid but low-value step (e.g., restating information or stalling) that adds minimal
 212 insight.
- 213 • `BAD`: A logically flawed, incoherent, or hallucinated step that leads the solution astray.

214 We analyzed the distribution of confidence gains (C_k) for each category. As illustrated in Figure
 215 2-(a), we observe a strict trend:

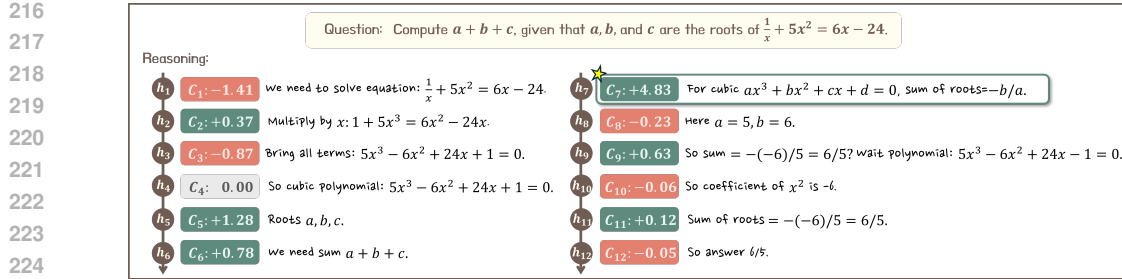


Figure 3: **Qualitative example of a pivotal step.** Among the reasoning steps, a critical insight at step h_7 (the introduction of Vieta’s formulas for a cubic equation) results in a large, distinct spike in the ground-truth confidence gain ($C_7 = +4.83$). This is substantially larger than the gains from more routine algebraic steps. Further qualitative examples are provided in Appendix E.

$$\text{Avg } C_k(\text{GREAT or OKAY}) > \text{Avg } C_k(\text{BAD})$$

The analysis shows that **GREAT** or **OKAY** steps, on average, drive ground-truth confidence upward, whereas **BAD** steps fail to contribute valid evidence, resulting in negligible or negative gains. This validates C_k as a dense, high-resolution signal capable of penalizing local errors and rewarding critical insights, a distinction that standard sparse outcome-based rewards fail to capture.

b) Causal Utility: Does guiding generation with this bias improve accuracy during inference?

To establish that confidence growth actively *guides* the reasoning process toward correctness, we utilized the stepwise confidence gain (C_k) as a scoring function for **test-time search**.

We implemented a **beam search with a beam width of 1**. At each reasoning step, we sampled $N = 8$ candidate extensions and greedily selected the single path maximizing the confidence gain C_k to continue generation. **We note that since C_k relies on the ground truth, this experiment serves purely as an analytical validation of the reward signal, not as a proposed inference method.**

We evaluated this approach across multiple sampling temperatures ($T \in \{0.8, 0.9, 1.0\}$). As shown in **Figure 2-(b)**, this confidence-guided search consistently outperforms the standard sampling baseline across all temperature settings. These results indicate that C_k serves as a robust steering signal, providing the dense supervision needed to differentiate valid paths from incorrect ones regardless of generation stochasticity. Crucially, this validates the confidence growth as a reinforcement learning reward: since the signal successfully guides the model to the correct solution when available, optimizing it during training encourages the model to intrinsically internalize this reasoning behavior.

Large Stepwise Confidence Gains Pinpoint Pivotal Reasoning Steps. Beyond the overall trend of confidence, we investigated whether the *magnitude* of the stepwise gain, C_k , correlates with the importance of individual reasoning steps. Qualitatively, we observe that large, positive spikes in C_k often coincide with pivotal moments in the reasoning process, such as the application of a key theorem or a critical insight. For instance, as illustrated in Figure 3, a step introducing the sum of roots formula for a cubic equation yields a substantially larger confidence gain compared to adjacent steps involving routine algebraic manipulation. To validate this rigorously, we conducted a quantitative pairwise comparison. For trajectories in $\mathcal{T}_{\text{correct}}$, we randomly sampled pairs of reasoning steps, h_i and h_j , under the condition that $C_i > C_j$. We then prompted an LLM evaluator (GPT-5) to judge which of the two steps was more critical for reaching the final solution (see Appendix D for detailed evaluation prompts). The step with the higher confidence gain, h_i , was frequently identified as more critical, achieving a win rate significantly above chance (Figure 4). This finding suggests that the magnitude of the confidence gain is not arbitrary; it is a meaningful signal that effectively pinpoints influential steps within a reasoning chain.

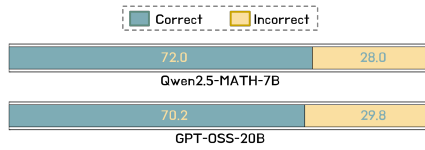


Figure 4: **Quantitative validation of step importance.** In a pairwise comparison, an LLM evaluator judged the step with the higher confidence gain ($C_i > C_j$) as more critical with a win rate significantly above chance, confirming that gain magnitude correlates with step importance.

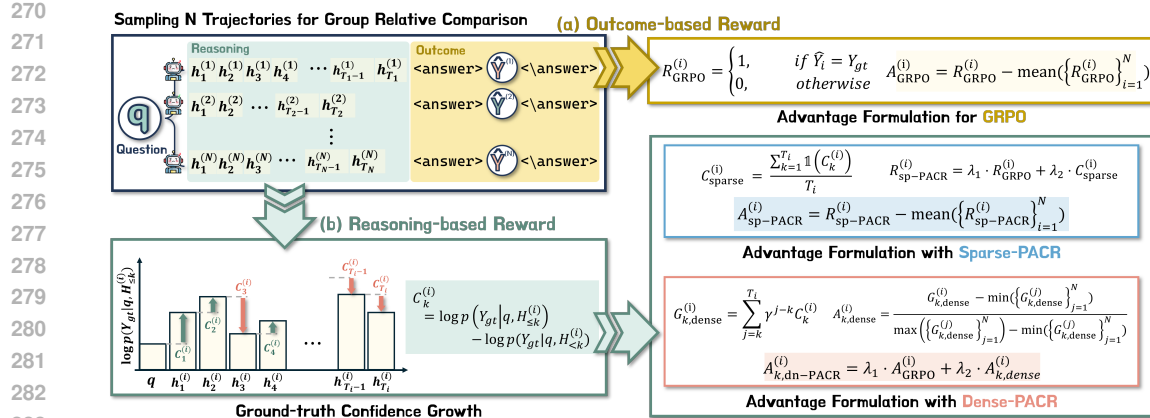


Figure 5: Overview of the PACR method and its integration with GRPO. Standard GRPO begins by sampling a group of N reasoning trajectories for a given question. (a) A standard outcome-based reward ($R_{GRPO}^{(i)}$) is calculated based on the correctness of the final answer. (b) Our proposed reasoning-based reward is derived from the ground-truth confidence growth ($C_k^{(i)}$) at each step. This signal is integrated into the final advantage calculation in two ways: **Sparse-PACR** uses the consistency of confidence growth to compute a single reward for the entire trajectory, while **Dense-PACR** uses the magnitude of each step’s gain to compute a fine-grained, per-step advantage.

5 METHOD: PROGRESSIVELY ASCENDING CONFIDENCE REWARD (PACR)

Based on our findings in Section 4, we now formalize how to incorporate the principle of ascending ground-truth confidence into the GRPO framework. To do this, we introduce the Progressively Ascending Confidence Reward (PACR), a procedural reward signal designed to complement the final outcome-based reward. We propose *two* variants: (1) **Sparse-PACR**, which applies a holistic, trajectory-level reward based on the consistency of confidence growth, and (2) **Dense-PACR**, which provides a fine-grained, step-wise reward based on the magnitude of each confidence change.

Sparse-PACR. In the Sparse setting, we compute a single procedural reward for an entire trajectory based on the consistency of its confidence growth. This reward, $C_{\text{sparse}}^{(i)}$, is the proportion of reasoning steps that produce a positive confidence gain. We calculate it using an indicator function, $\mathbb{I}(\cdot)$:

$$C_{\text{sparse}}^{(i)} = \frac{1}{T_i} \sum_{k=1}^{T_i} \mathbb{I}(C_k^{(i)} > 0), \quad (7)$$

where $C_k^{(i)}$ is the confidence gain in Eq. 6. The final reward for trajectory i , $R_{\text{sp-PACR}}^{(i)}$, is a weighted combination of the standard outcome-based reward, $R_{GRPO}^{(i)}$, and our sparse procedural reward:

$$R_{\text{sp-PACR}}^{(i)} = \lambda_1 \cdot R_{GRPO}^{(i)} + \lambda_2 \cdot C_{\text{sparse}}^{(i)}. \quad (8)$$

This combined reward is then used to calculate the trajectory’s advantage, $A_{\text{sp-PACR}}^{(i)}$, within the GRPO framework by centering it against the group average:

$$A_{\text{sp-PACR}}^{(i)} = R_{\text{sp-PACR}}^{(i)} - \text{mean}(\{R_{\text{sp-PACR}}^{(j)}\}_{j=1}^N). \quad (9)$$

Dense-PACR. The Dense setting provides a more granular, step-wise reward signal. At each reasoning step k in trajectory i , we use the ground-truth confidence gain, $C_k^{(i)}$, as an immediate reward. From this, we compute the discounted return for that step, $G_{k,\text{dense}}^{(i)}$, by summing the rewards from that point forward:

$$G_{k,\text{dense}}^{(i)} = \sum_{j=k}^{T_i} \gamma^{j-k} C_j^{(i)}, \quad (10)$$

324 where γ is a discount factor. To create a stable, step-wise advantage signal, $A_{k,\text{dense}}^{(i)}$, we normalize
 325 these returns across the group at each step k . Specifically, we use Min-Max scaling to map the returns
 326 to a $[0, 1]$ range. This creates a purely positive signal that only incentivizes confidence growth without
 327 penalizing steps that do not, a design choice we validate in our ablations (Section 7.5). To handle
 328 trajectories of varying lengths, the discounted return $G_{k,\text{dense}}^{(i)}$ is treated as zero for any step k that
 329 does not exist in trajectory i . The resulting advantage for a step k in trajectory i is then:
 330

$$A_{k,\text{dense}}^{(i)} = \frac{G_{k,\text{dense}}^{(i)} - \min_j(\{G_{k,\text{dense}}^{(j)}\}_{j=1}^N)}{\max_j(\{G_{k,\text{dense}}^{(j)}\}_{j=1}^N) - \min_j(\{G_{k,\text{dense}}^{(j)}\}_{j=1}^N)}. \quad (11)$$

335 Finally, the total advantage at each step, $A_{k,\text{dn-PACR}}^{(i)}$, is the weighted sum of the trajectory-level GRPO
 336 advantage and our dense, step-wise advantage:
 337

$$A_{k,\text{dn-PACR}}^{(i)} = \lambda_1 \cdot A_{\text{GRPO}}^{(i)} + \lambda_2 \cdot A_{k,\text{dense}}^{(i)}, \quad (12)$$

339 where $A_{\text{GRPO}}^{(i)} = R_{\text{GRPO}}^{(i)} - \text{mean}(\{R_{\text{GRPO}}^{(j)}\}_{j=1}^N)$. This final advantage is then used to update the policy.
 340

342 6 EXPERIMENTAL SETUP

344 **Models and Baselines.** We experiment with three open-source LLMs: Qwen2.5-Math-1.5B,
 345 Qwen2.5-Math-7B (Yang et al., 2024), and Qwen3-4B¹ (Yang et al., 2025a). Our baseline for
 346 all experiments is Dr.GRPO (Liu et al., 2025b), a bias-mitigated version of GRPO (Shao et al.,
 347 2024b), which we implement using the OAT framework (Liu et al., 2024). We compare this baseline
 348 against our two proposed methods, Sparse-PACR and Dense-PACR.
 349

350 **Datasets and Evaluation.** For training, we use the MATH dataset (Hendrycks et al.). Following
 351 prior work (Liu et al., 2025b), we use the full dataset for the 1.5B model and filter for the more
 352 challenging levels (3-5) for the 4B and 7B models. To evaluate performance, we test our models
 353 on five diverse mathematical reasoning benchmarks: MATH500 (Hendrycks et al.), Minerva-Math
 354 (Lewkowycz et al., 2022), OlympiadBench (He et al., 2024), AIME 2024, and AMC 2023 (Li et al.,
 355 2024a). Final answers are programmatically checked for correctness using the Math-Verify (Kydlíček,
 356 2025) library. All results are reported as pass@1 using greedy decoding (temperature of 0).
 357

358 **Training Details.** For each problem, we generate a group of 8 responses using sampling with a
 359 temperature of 1.0. We report the average results across three runs with different random seeds for
 360 all experiments. All models were trained on a single node with $8 \times$ NVIDIA H100 80GB GPUs.
 361 Further details on hyperparameters, such as learning rate and batch size, are provided in Appendix C.
 362

363 7 RESULTS AND ABLATIONS

364 7.1 EXPERIMENTAL RESULT

366 Table 1 presents the quantitative results on various math benchmarks. For the Qwen2.5-series, we also
 367 include the instruct models at the sample scale and R1-Distill models for comparison by following
 368 (Liu et al., 2025b). Our proposed reward, PACR, demonstrates significant improvements over the
 369 outcome-based reward baseline (+Dr.GRPO) in both its Sparse and Dense setting. This shows that
 370 our core method provides a positive inductive bias for improving the reasoning skills of language
 371 models.
 372

373 While the sparse trajectory-level reward, Sparse-PACR, is effective on its own, we observe that
 374 Dense-PACR, which provides a more fine-grained reward, consistently achieves better performance.
 375 This highlights that enriching the training process with a dense reward signal allows the model to
 376 learn from more detailed feedback, leading to further gains in its reasoning capabilities.
 377

¹For the Qwen3-4B model, we set ‘enable_thinking=False’ to disable its built-in chain-of-thought capabilities, allowing for a direct comparison of how our method versus standard GRPO teaches this capability.

378 Table 1: **Results on reasoning benchmarks.** We report pass@1 accuracy using temperature $T = 0.0$
379 across six benchmarks. Both Sparse-PACR and Dense-PACR consistently outperform the Dr.GRPO
380 baseline across all model sizes. \dagger is marked for the score reproduced and other baseline scores are
381 from Liu et al. (2025b). The green colored numbers in the Average column indicate the absolute
382 performance improvement over the Dr.GRPO baseline.

Base model + Method	AIME25	AIME24	AMC	MATH500	Minerva	OlympiadBench	Average
R1-distill-Qwen-1.5B (Gen. length 8k)	13.3	10.0	40.9	54.6	9.2	24.1	25.4
R1-distill-Qwen-1.5B + Dr.GRPO \dagger	16.7	20.0	50.6	75.2	24.3	34.4	36.9
R1-distill-Qwen-1.5B + Sparse-PACR	20.0	16.7	53.0	76.8	29.4	37.8	38.9 ± 2.0
R1-distill-Qwen-1.5B + Dense-PACR	20.0	20.0	56.6	78.0	26.5	38.8	40.0 ± 3.1
Qwen2.5-Math-1.5B	3.3	20.0	32.5	33.0	12.5	22.8	20.7
R1-Distill-Qwen-1.5B (Gen. length 3k)	10.0	2.5	21.7	52.2	16.3	17.3	20.0
Qwen2.5-Math-1.5B-Instruct	10.0	10.0	48.2	74.2	26.5	40.2	34.8
Qwen2.5-Math-1.5B + Dr.GRPO \dagger	6.7	13.3	47.0	76.8	32.3	39.0	35.8
Qwen2.5-Math-1.5B + Sparse-PACR	13.3	20.0	48.4	77.4	29.4	37.8	37.7 ± 1.9
Qwen2.5-Math-1.5B + Dense-PACR	13.3	23.3	49.4	77.4	31.7	39.0	39.0 ± 3.2
Qwen2.5-Math-7B	6.7	16.7	38.6	50.6	9.9	16.6	23.2
SimpleRL-Zero-7B	6.7	26.7	60.2	78.2	27.6	40.3	39.95
PRIME-Zero-7B	16.7	16.7	62.7	83.8	36.0	40.9	42.8
OpenReasoner-Zero- 7B @ 3k	3.3	13.3	47.0	79.2	31.6	44.0	36.4
R1-Distill-Qwen-7B @ 3k	20.0	10.0	26.2	60.1	23.0	23.1	27.1
Qwen2.5-Math-7B-Instruct	16.7	16.7	53.0	83.6	29.8	42.7	40.4
Qwen2.5-Math-7B + Dr.GRPO \dagger	13.3	30.0	56.6	81.8	34.6	45.2	43.6
Qwen2.5-Math-7B + Sparse-PACR	13.3	36.7	55.4	82.6	34.6	45.6	44.7 ± 1.1
Qwen2.5-Math-7B + Dense-PACR	16.7	43.3	56.1	81.9	35.6	46.1	46.6 ± 3.0
Qwen3-4B	6.7	13.3	32.5	40.2	9.19	39.4	23.5
Qwen3-4B + Dr.GRPO \dagger	20.0	40.0	63.8	88.4	33.8	46.8	48.8
Qwen3-4B + Sparse-PACR	20.0	33.3	67.5	86.2	35.3	54.4	49.4 ± 0.7
Qwen3-4B + Dense-PACR	26.7	46.7	63.4	86.8	36.0	55.0	52.4 ± 3.6

400
401 Table 2: **Results on Pass@k.** Using temperature $T = 1.0$, Pass@1 (n=16) is calculated as the
402 average accuracy across 16 sampled trajectories, while Pass@16 represents the probability that at
403 least one of the 16 samples is correct. The green colored numbers in the Average column indicate the
404 absolute performance improvement over the Dr.GRPO baseline.

Base model + Method	Metric	AIME25	AIME24	AMC	MATH500	Minerva	OlympiadBench	Average
Qwen3-4B	pass@1 (n=16)	7.9	8.9	30.7	66.5	25.2	27.0	27.7
Qwen3-4B + Dr.GRPO	pass@1 (n=16)	21.0	24.6	61.4	85.6	33.0	53.8	46.4
Qwen3-4B + Dense-PACR	pass@1 (n=16)	30.2	30.0	66.5	86.8	33.8	56.2	50.6 ± 4.2
Qwen3-4B	pass@16	16.7	33.3	48.2	82.8	37.9	41.6	43.4
Qwen3-4B + Dr.GRPO	pass@16	40.0	50.0	84.3	94.4	46.7	70.4	64.3
Qwen3-4B + Dense-PACR	pass@16	46.7	56.7	84.3	94.8	48.9	71.1	67.1 ± 2.8

7.2 SAMPLING EFFICIENCY AND INTRINSIC REASONING CAPABILITY

413 A critical question in RL is whether performance gains stem from genuine reasoning improvement or
414 merely optimized sampling efficiency (i.e., narrowing the distribution around easy solutions at the
415 expense of diversity) (Yue et al., 2025; Kirk et al., 2023; Yu, 2025). To distinguish these effects, we
416 evaluate our models with a positive sampling temperature ($T = 1.0$), reporting two metrics: **Pass@1**
417 (**n=16**) as a proxy for *sampling efficiency* (sharpening probability on correct paths), and **Pass@16** as
418 a proxy for *intrinsic capability* (expanding the manifold of solvable problems).

419 As shown in Table 2, Dense-PACR consistently outperforms the baseline on both fronts. The gain in
420 **Pass@1** confirms improved efficiency, while the concurrent rise in **Pass@16** demonstrates a genuine
421 expansion of reasoning capability.

7.3 DISENTANGLING DENSE SUPERVISION FROM TRAINING STABILITY

425 A potential confounder for PACR’s performance is the mitigation of the vanishing advantage problem.
426 In standard GRPO, if all N sampled trajectories share the same outcome (e.g., all incorrect), the
427 group-relative advantage collapses to zero, providing no learning signal. PACR naturally bypasses
428 this issue by assigning continuous, dense rewards (C_k) that differentiate trajectories even when final
429 outcomes are identical.

431 To disentangle the benefits of dense supervision from simple gradient stability, we implemented the
432 **dynamic sampling** strategy from DAPO (Yu et al., 2025) as a baseline. This method resolves the

432
 433 Table 3: **Comparison with Dynamic Sampling (Stability Baseline).** To isolate the benefit of dense
 434 supervision from training stability, we integrated the dynamic sampling strategy from DAPO (Yu
 435 et al., 2025). The green colored numbers in the Average column indicate the absolute performance
 436 improvement over the Dr.GRPO baseline.

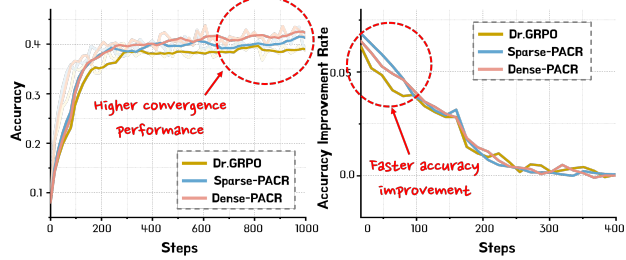
Base model + Method	AIME25	AIME24	AMC	MATH500	Minerva	OlympiadBench	Average
R1-Distill-Qwen-1.5B (Gen. length 8k)	13.3	10.0	40.9	54.6	9.2	24.1	25.4
+ Dr.GRPO	16.7	20.0	50.6	75.2	24.3	34.4	36.8
+ Dr.GRPO + Dynamic Sampling	10.0	20.0	60.2	79.6	28.9	40.4	39.0 <small>+2.2</small>
+ Dense-PACR	20.0	20.0	56.6	78.0	26.5	38.8	40.0 <small>+3.2</small>
+ Dense-PACR + Dynamic Sampling	16.7	26.7	56.6	80.6	25.7	37.3	40.6 <small>+3.8</small>

440
 441 vanishing advantage by resampling trajectories until the group contains diverse outcomes, such that it
 442 maintains the effective batch size across the training.

443 Table 3 presents the results. While dynamic sampling indeed boosts the Dr.GRPO baseline (raising
 444 accuracy from 36.8% to 39.0%), Dense-PACR (40.0%) consistently outperforms this stabilized
 445 baseline. Furthermore, combining both methods yields the highest performance (40.6%). This
 446 performance gap confirms that stability alone cannot explain the gains; rather, the confidence growth
 447 signal (C_k) provides necessary directional guidance, steering the model toward better reasoning
 448 beyond mere gradient stabilization.

451 7.4 TRAINING CURVE: PACR ACCELERATES EXPLORATION AND IMPROVES CONVERGENCE

452 Figure 6 illustrates the training dynamics, plotting the average pass@1 accuracy over training steps (left) and
 453 the corresponding rate of accuracy improvement (right). The right plot highlights that both PACR variants
 454 have a significantly higher rate of improvement compared to the Dr.GRPO baseline, especially during the critical
 455 early exploration phase of RL training. As shown on the left, this accelerated learning ultimately allows the PACR
 456 methods to converge to a higher final accuracy.



457 Figure 6: **Training dynamics for Qwen2.5-Math-1.5B.** Average pass@1 accuracy (left) and rate of accuracy improvement (right) during training. PACR methods show a faster initial rate of improvement, accelerating exploration and converging to a higher final performance.

466 7.5 ANALYSIS ON ADVANTAGE FORMULATION: IMPACT OF PENALIZING INTERMEDIATE 467 STEPS

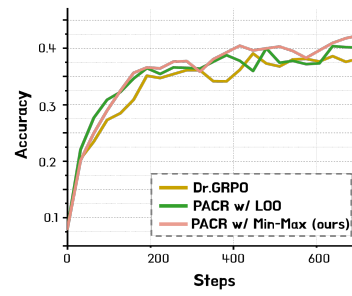
468 In this section, we analyze the impact of the advantage
 469 formulation in our Dense-PACR setting. A crucial design
 470 choice is how to normalize the raw discounted returns
 471 ($G_{k,\text{dense}}^{(i)}$) into a stable advantage signal. We compare our
 472 Min-Max normalization against a widely used Leave-One-
 473 Out (LOO) baseline (Ahmadian et al., 2024; Cui et al.,
 474 2025).

475 The key difference is that the LOO baseline centers the re-
 476 turns, which can assign **negative advantages** that penalize
 477 steps with below-average confidence gains:

$$478 A_{k,\text{loo}}^{(i)} = G_{k,\text{dense}}^{(i)} - \text{mean}(\{G_{k,\text{dense}}^{(j)}\}_{j=1, j \neq i}^N). \quad (13)$$

479 In contrast, our Min-Max normalization (Eq. 11) scales returns to a $[0, 1]$ range, creating a **purely**
 480 **positive signal** for the reasoning process that only rewards confidence growth.

481 Figure 7 shows this design choice has a clear impact on the training dynamics. The penalizing nature
 482 of the LOO baseline initially accelerates learning by aggressively pruning suboptimal steps, but this



483 Figure 7: **Advantage Normalization.** Comparison of Min-Max and Leave-
 484 One-Out (LOO) for Dense-PACR on
 485 Qwen2.5-Math-1.5B.

486
 487 Table 4: **Results on Logical Reasoning Benchmarks.** We report pass@1 accuracy using temperature
 488 $T = 0.0$ across two benchmarks.

489 Base model + Method	490 K-K				491 ZebraLogic					
	492 ppl6	493 ppl7	494 ppl8	495 Avg.	496 Small	497 Medium	498 Large	499 X-Large	500 Grid Acc.	501 Cell Acc.
496 Qwen-3-4B	497 94.0	498 89.0	499 85.0	500 89.3	501 99.4	502 94.3	503 61.0	504 11.5	505 57.8	506 72.7
497 Qwen-3-4B + Dr.GRPO	498 89.0	499 82.0	500 79.0	501 83.8	502 98.4	503 92.9	504 59.5	505 8.5	506 56.11	507 71.1
498 Qwen-3-4B + PACR	499 93.0	500 95.0	501 87.0	502 91.7	503 99.1	504 95.4	505 65.5	506 11.0	507 58.2	508 73.7

493
 494 leads to premature convergence and a performance plateau. Conversely, our non-penalizing Min-Max
 495 approach encourages more sustained exploration, ultimately converging to a higher final accuracy.
 496 With our method, process-level penalization is avoided; a negative training signal is only applied by
 497 the main GRPO reward when the model produces a definitively incorrect final answer.
 498

500 7.6 ANALYSIS ON COMPUTATION OVERHEAD

501 A natural concern with dense rewards is the com-
 502 putational overhead incurred by calculating C_k
 503 at every reasoning step. While these values are
 504 computed via batched forward passes, the num-
 505 ber of required passes scales linearly with gen-
 506 eration length, inevitably increasing the wall-clock
 507 time per training iteration compared to the stan-
 508 dard sparse reward baseline.

509 To quantify this trade-off, we compare the train-
 510 ing efficiency in Figure 8. As shown in Figure 8-
 511 (a), PACR indeed incurs a higher computational
 512 cost per step compared to the sparse baseline
 513 (Dr.GRPO). However, Figure 8-(b) demon-
 514 strates that in terms of **Time-to-Convergence**, PACR
 515 is more efficient. When accuracy is analyzed as a
 516 function of total wall-clock training time, the PACR
 517 curve lies above the baseline. This indicates that the
 518 acceleration in learning provided by the dense
 519 signal effectively outweighs the overhead of the addi-
 520 tional forward passes.

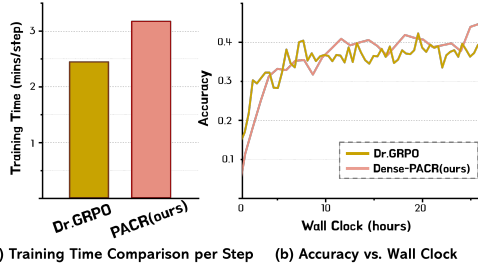
521 7.7 EXPAND TO LOGICAL REASONING

522 To test the generalization of our method beyond mathematics, we expanded our experimental scope to
 523 the domain of logical reasoning. We explicitly trained our models on Knights and Knaves (K-K) train
 524 set Xie et al. (2024), utilizing the verifiable version preprocessed by Xie et al. (2025). We evaluate on
 525 the test set of K-K and ZebraLogic (Lin et al., 2024) benchmark.

526 As shown in Table 4, this domain poses a unique challenge for standard RL: the Dr.GRPO baseline
 527 exhibits performance degradation compared to the base model (e.g., K-K Average drops from 89.3%
 528 to 83.8%), suggesting that sparse rewards are insufficient for credit assignment in brittle logical
 529 chains. In contrast, **PACR recovers and exceeds the base model’s performance** (e.g., 91.7% on
 530 K-K).

531 8 CONCLUSION

532 In this work, we addressed the limitations of sparse, outcome-based rewards in RLVR by introducing
 533 the Progressively Ascending Confidence Reward (PACR), a dense, model-intrinsic signal derived from
 534 the model’s evolving belief in the ground-truth answer. Through a series of empirical observations and
 535 a formal theoretical proof, we validated that confidence growth serves as a powerful inductive bias,
 536 effectively constraining the search space to regions richer in logically sound and faithful reasoning
 537 paths. Our experiments demonstrated that augmenting GRPO with PACR not only accelerates
 538 training but also converges to a higher final performance across multiple reasoning benchmarks,
 539 with the fine-grained Dense-PACR variant proving most effective. Ultimately, our work shows that
 540 informative, dense rewards for complex reasoning can be effectively extracted from the internal
 541 dynamics of the learning policy itself, suggesting a promising direction for creating more effective
 542 and reliable methods for fine-tuning the reasoning capabilities of large language models.



543 Figure 8: **Computation Overhead on Qwen2.5-
 544 Math-1.5B.**

545 (a) Training Time Comparison per Step (b) Accuracy vs. Wall Clock

546

547

548

549

550

551

552

553

554

555

556

557

558

559

560

561

562

563

564

565

566

567

568

569

570

571

572

573

574

575

576

577

578

579

580

581

582

583

584

585

586

587

588

589

590

591

592

593

594

595

596

597

598

599

600

601

602

603

604

605

606

607

608

609

610

611

612

613

614

615

616

617

618

619

620

621

622

623

624

625

626

627

628

629

630

631

632

633

634

635

636

637

638

639

640

641

642

643

644

645

646

647

648

649

650

651

652

653

654

655

656

657

658

659

660

661

662

663

664

665

666

667

668

669

670

671

672

673

674

675

676

677

678

679

680

681

682

683

684

685

686

687

688

689

690

691

692

693

694

695

696

697

698

699

700

701

702

703

704

705

706

707

708

709

710

711

712

713

714

715

716

717

718

719

720

721

722

723

724

725

726

727

728

729

730

731

732

733

734

735

736

737

738

739

740

741

742

743

744

745

746

747

748

749

750

751

752

753

754

755

756

757

758

759

760

761

762

763

764

765

766

767

540 REFERENCES
541

542 Arash Ahmadian, Chris Cremer, Matthias Gallé, Marzieh Fadaee, Julia Kreutzer, Olivier Pietquin,
543 Ahmet Üstün, and Sara Hooker. Back to basics: Revisiting reinforce-style optimization for learning
544 from human feedback in llms. In *Proceedings of the 62nd Annual Meeting of the Association for
545 Computational Linguistics (Volume 1: Long Papers)*, pp. 12248–12267, 2024.

546 Yuntao Bai, Andy Jones, Kamal Ndousse, Amanda Askell, Anna Chen, Nova DasSarma, Dawn Drain,
547 Stanislav Fort, Deep Ganguli, Tom Henighan, et al. Training a helpful and harmless assistant with
548 reinforcement learning from human feedback. *arXiv preprint arXiv:2204.05862*, 2022.

549 Meng Cao, Lei Shu, Lei Yu, Yun Zhu, Nevan Wicher, Yinxiao Liu, and Lei Meng. Drlc: Reinforce-
550 ment learning with dense rewards from llm critic, 2024.

551 Alex J Chan, Hao Sun, Samuel Holt, and Mihaela Van Der Schaar. Dense reward for free in
552 reinforcement learning from human feedback. In *Proceedings of the 41st International Conference
553 on Machine Learning*, pp. 6136–6154, 2024.

554 Wenhua Chen, Xueguang Ma, Xinyi Wang, and William W Cohen. Program of thoughts prompting:
555 Disentangling computation from reasoning for numerical reasoning tasks. *arXiv preprint
556 arXiv:2211.12588*, 2022.

557 Jie Cheng, Ruixi Qiao, Lijun Li, Chao Guo, Junle Wang, Gang Xiong, Yisheng Lv, and Fei-Yue Wang.
558 Stop summation: Min-form credit assignment is all process reward model needs for reasoning.
559 *arXiv preprint arXiv:2504.15275*, 2025.

560 Gheorghe Comanici, Eric Bieber, Mike Schaeckermann, Ice Pasupat, Noveen Sachdeva, Inderjit
561 Dhillon, Marcel Blstein, Ori Ram, Dan Zhang, Evan Rosen, et al. Gemini 2.5: Pushing the frontier
562 with advanced reasoning, multimodality, long context, and next generation agentic capabilities.
563 *arXiv preprint arXiv:2507.06261*, 2025.

564 Ganqu Cui, Lifan Yuan, Zefan Wang, Hanbin Wang, Wendi Li, Bingxiang He, Yuchen Fan, Tianyu
565 Yu, Qixin Xu, Weize Chen, et al. Process reinforcement through implicit rewards. *arXiv preprint
566 arXiv:2502.01456*, 2025.

567 Luyu Gao, Aman Madaan, Shuyan Zhou, Uri Alon, Pengfei Liu, Yiming Yang, Jamie Callan, and
568 Graham Neubig. Pal: Program-aided language models. In *International Conference on Machine
569 Learning*, pp. 10764–10799. PMLR, 2023.

570 Zhibin Gou, Zhihong Shao, Yeyun Gong, Yelong Shen, Yujiu Yang, Minlie Huang, Nan Duan, and
571 Weizhu Chen. Tora: A tool-integrated reasoning agent for mathematical problem solving. *arXiv
572 preprint arXiv:2309.17452*, 2023.

573 Daya Guo, Dejian Yang, Haowei Zhang, Junxiao Song, Ruoyu Zhang, Runxin Xu, Qihao Zhu,
574 Shirong Ma, Peiyi Wang, Xiao Bi, et al. Deepseek-r1: Incentivizing reasoning capability in llms
575 via reinforcement learning. *arXiv preprint arXiv:2501.12948*, 2025.

576 John Hale. A probabilistic earley parser as a psycholinguistic model. In *North American Chapter of the
577 Association for Computational Linguistics*, 2001. URL <https://api.semanticscholar.org/CorpusID:5490143>.

578 Chaoqun He, Renjie Luo, Yuzhuo Bai, Shengding Hu, Zhen Thai, Junhao Shen, Jinyi Hu, Xu Han,
579 Yujie Huang, Yuxiang Zhang, et al. Olympiadbench: A challenging benchmark for promoting
580 agi with olympiad-level bilingual multimodal scientific problems. In *Proceedings of the 62nd
581 Annual Meeting of the Association for Computational Linguistics (Volume 1: Long Papers)*, pp.
582 3828–3850, 2024.

583 Dan Hendrycks, Collin Burns, Saurav Kadavath, Akul Arora, Steven Basart, Eric Tang, Dawn Song,
584 and Jacob Steinhardt. Measuring mathematical problem solving with the math dataset. *Sort*, 2(4):
585 0–6.

586 Jingcheng Hu, Yinmin Zhang, Qi Han, Dixin Jiang, Xiangyu Zhang, and Heung-Yeung Shum.
587 Open-reasoner-zero: An open source approach to scaling up reinforcement learning on the base
588 model. *arXiv preprint arXiv:2503.24290*, 2025.

594 Robert Kirk, Ishita Mediratta, Christoforos Nalmpantis, Jelena Luketina, Eric Hambro, Edward
 595 Grefenstette, and Roberta Raileanu. Understanding the effects of rlhf on llm generalisation and
 596 diversity. *arXiv preprint arXiv:2310.06452*, 2023.

597

598 Aviral Kumar, Vincent Zhuang, Rishabh Agarwal, Yi Su, John D Co-Reyes, Avi Singh, Kate Baumli,
 599 Shariq Iqbal, Colton Bishop, Rebecca Roelofs, et al. Training language models to self-correct via
 600 reinforcement learning. In *The Thirteenth International Conference on Learning Representations*.

601 Hynek Kydlíček. Math-Verify: Math Verification Library, 2025. URL <https://github.com/huggingface/math-verify>.

602

603 Dong Bok Lee, Seanie Lee, Sangwoo Park, Minki Kang, Jinheon Baek, Dongki Kim, Dominik
 604 Wagner, Jiongdao Jin, Heejun Lee, Tobias Bocklet, et al. Rethinking reward models for multi-
 605 domain test-time scaling. *arXiv preprint arXiv:2510.00492*, 2025.

606

607 Roger Levy. Expectation-based syntactic comprehension. *Cognition*, 106(3):1126–1177, 2008.
 608 ISSN 0010-0277. doi: <https://doi.org/10.1016/j.cognition.2007.05.006>. URL <https://www.sciencedirect.com/science/article/pii/S0010027707001436>.

609

610 Aitor Lewkowycz, Anders Andreassen, David Dohan, Ethan Dyer, Henryk Michalewski, Vinay Ra-
 611 masesh, Ambrose Slone, Cem Anil, Imanol Schlag, Theo Gutman-Solo, et al. Solving quantitative
 612 reasoning problems with language models. *Advances in neural information processing systems*,
 613 35:3843–3857, 2022.

614

615 Jia Li, Edward Beeching, Lewis Tunstall, Ben Lipkin, Roman Soletskyi, Shengyi Huang, Kashif
 616 Rasul, Longhui Yu, Albert Q Jiang, Ziju Shen, et al. Numinamath: The largest public dataset in
 617 ai4maths with 860k pairs of competition math problems and solutions. *Hugging Face repository*,
 13(9):9, 2024a.

618

619 Wendi Li and Yixuan Li. Process reward model with q-value rankings. In *The Thirteenth International
 620 Conference on Learning Representations*, 2025. URL <https://openreview.net/forum?id=wQEdh2cgEk>.

621

622 Ziniu Li, Tian Xu, Yushun Zhang, Zhihang Lin, Yang Yu, Ruoyu Sun, and Zhi-Quan Luo. Remax: a
 623 simple, effective, and efficient reinforcement learning method for aligning large language models.
 624 In *Proceedings of the 41st International Conference on Machine Learning*, pp. 29128–29163,
 625 2024b.

626

627 Hunter Lightman, Vineet Kosaraju, Yuri Burda, Harrison Edwards, Bowen Baker, Teddy Lee, Jan
 628 Leike, John Schulman, Ilya Sutskever, and Karl Cobbe. Let's verify step by step. In *The Twelfth
 629 International Conference on Learning Representations*, 2023.

630

631 Bill Yuchen Lin, Ronan Le Bras, and Yejin Choi. ZebraLogic: Benchmarking the logical reasoning
 632 ability of language models, 2024. URL <https://huggingface.co/spaces/allenai/ZebraLogic>.

633

634 Aiwei Liu, Haoping Bai, Zhiyun Lu, Yanchao Sun, Xiang Kong, Xiaoming Simon Wang, Jiulong
 635 Shan, Albin Madappally Jose, Xiaojiang Liu, Lijie Wen, et al. Tis-dpo: Token-level importance
 636 sampling for direct preference optimization with estimated weights. In *The Thirteenth International
 637 Conference on Learning Representations*.

638

639 Yuliang Liu, Junjie Lu, Zhaoling Chen, Chaofeng Qu, Jason Klein Liu, Chonghan Liu, Zefan Cai,
 640 Yunhui Xia, Li Zhao, Jiang Bian, et al. Adaptivestep: Automatically dividing reasoning step
 641 through model confidence. *arXiv preprint arXiv:2502.13943*, 2025a.

642

643 Zichen Liu, Changyu Chen, Xinyi Wan, Chao Du, Wee Sun Lee, and Min Lin. Oat: A research-
 644 friendly framework for llm online alignment, 2024.

645

646 Zichen Liu, Changyu Chen, Wenjun Li, Penghui Qi, Tianyu Pang, Chao Du, Wee Sun Lee, and Min
 647 Lin. Understanding r1-zero-like training: A critical perspective. *arXiv preprint arXiv:2503.20783*,
 648 2025b.

649

650 Ilya Loshchilov and Frank Hutter. Decoupled weight decay regularization. In *International Confer-
 651 ence on Learning Representations*, 2017.

648 Long Ouyang, Jeffrey Wu, Xu Jiang, Diogo Almeida, Carroll Wainwright, Pamela Mishkin, Chong
 649 Zhang, Sandhini Agarwal, Katarina Slama, Alex Ray, et al. Training language models to follow
 650 instructions with human feedback. *Advances in neural information processing systems*, 35:27730–
 651 27744, 2022.

652 Rafael Rafailov, Joey Hejna, Ryan Park, and Chelsea Finn. From r to q^* : Your language model is
 653 secretly a q -function. In *First Conference on Language Modeling*.

654 Rafael Rafailov, Archit Sharma, Eric Mitchell, Christopher D Manning, Stefano Ermon, and Chelsea
 655 Finn. Direct preference optimization: Your language model is secretly a reward model. *Advances*
 656 *in neural information processing systems*, 36:53728–53741, 2023.

657 John Schulman, Filip Wolski, Prafulla Dhariwal, Alec Radford, and Oleg Klimov. Proximal policy
 658 optimization algorithms. *arXiv preprint arXiv:1707.06347*, 2017.

659 Zhihong Shao, Peiyi Wang, Qihao Zhu, Runxin Xu, Junxiao Song, Xiao Bi, Haowei Zhang,
 660 Mingchuan Zhang, YK Li, Yang Wu, et al. Deepseekmath: Pushing the limits of mathematical
 661 reasoning in open language models. *arXiv preprint arXiv:2402.03300*, 2024a.

662 Zhihong Shao, Peiyi Wang, Qihao Zhu, Runxin Xu, Junxiao Song, Xiao Bi, Haowei Zhang,
 663 Mingchuan Zhang, YK Li, Yang Wu, et al. Deepseekmath: Pushing the limits of mathematical
 664 reasoning in open language models. *arXiv preprint arXiv:2402.03300*, 2024b.

665 Qwen Team. Qwq-32b: Embracing the power of reinforcement learning, March 2025. URL
 666 <https://qwenlm.github.io/blog/qwq-32b/>.

667 Jiaqi Wang, Kevin Qinghong Lin, James Cheng, and Mike Zheng Shou. Think or not? selective
 668 reasoning via reinforcement learning for vision-language models. *arXiv preprint arXiv:2505.16854*,
 669 2025.

670 Zeqiu Wu, Yushi Hu, Weijia Shi, Nouha Dziri, Alane Suhr, Prithviraj Ammanabrolu, Noah A. Smith,
 671 Mari Ostendorf, and Hannaneh Hajishirzi. Fine-grained human feedback gives better rewards for
 672 language model training. In *Thirty-seventh Conference on Neural Information Processing Systems*,
 673 2023. URL <https://openreview.net/forum?id=CSbGXyCswu>.

674 Chulin Xie, Yangsibo Huang, Chiyuan Zhang, Da Yu, Xinyun Chen, Bill Yuchen Lin, Bo Li, Badih
 675 Ghazi, and Ravi Kumar. On memorization of large language models in logical reasoning. 2024.
 676 URL <https://arxiv.org/abs/2410.23123>.

677 Tian Xie, Zitian Gao, Qingnan Ren, Haoming Luo, Yuqian Hong, Bryan Dai, Joey Zhou, Kai Qiu,
 678 Zhirong Wu, and Chong Luo. Logic-rl: Unleashing llm reasoning with rule-based reinforcement
 679 learning. *arXiv preprint arXiv:2502.14768*, 2025.

680 An Yang, Beichen Zhang, Binyuan Hui, Bofei Gao, Bowen Yu, Chengpeng Li, Dayiheng Liu, Jian-
 681 hong Tu, Jingren Zhou, Junyang Lin, et al. Qwen2. 5-math technical report: Toward mathematical
 682 expert model via self-improvement. *arXiv preprint arXiv:2409.12122*, 2024.

683 An Yang, Anfeng Li, Baosong Yang, Beichen Zhang, Binyuan Hui, Bo Zheng, Bowen Yu, Chang
 684 Gao, Chengan Huang, Chenxu Lv, et al. Qwen3 technical report. *arXiv preprint arXiv:2505.09388*,
 685 2025a.

686 Dayu Yang, Tianyang Liu, Daoan Zhang, Antoine Simoulin, Xiaoyi Liu, Yuwei Cao, Zhaopu Teng,
 687 Xin Qian, Grey Yang, Jiebo Luo, et al. Code to think, think to code: A survey on code-enhanced
 688 reasoning and reasoning-driven code intelligence in llms. *arXiv preprint arXiv:2502.19411*, 2025b.

689 Zhaohui Yang, Chenghua He, Xiaowen Shi, Linjing Li, Qiyue Yin, Shihong Deng, and Daxin Jiang.
 690 Beyond the first error: Process reward models for reflective mathematical reasoning. *arXiv preprint*
 691 *arXiv:2505.14391*, 2025c.

692 Zhaohui Yang, Chenghua He, Xiaowen Shi, Linjing Li, Qiyue Yin, Shihong Deng, and Daxin Jiang.
 693 Beyond the first error: Process reward models for reflective mathematical reasoning. *arXiv preprint*
 694 *arXiv:2505.14391*, 2025d.

702 Eunseop Yoon, Hee Suk Yoon, Soo Hwan Eom, Gunsoo Han, Daniel Wontae Nam, Daejin Jo,
 703 Kyoungho Woon On, Mark Hasegawa-Johnson, Sungwoong Kim, and Chang D Yoo. Tlcr: Token-
 704 level continuous reward for fine-grained reinforcement learning from human feedback. In *Findings*
 705 of the 62nd Annual Meeting of the Association for Computational Linguistics, ACL 2024, pp.
 706 14969–14981. Association for Computational Linguistics (ACL), 2024.

707 Hee Suk Yoon, Eunseop Yoon, Mark A Hasegawa-Johnson, Sungwoong Kim, and Chang D Yoo.
 708 Confpo: Exploiting policy model confidence for critical token selection in preference optimization.
 709 In *Forty-second International Conference on Machine Learning*.

710 Dian Yu, Baolin Peng, Ye Tian, Linfeng Song, Haitao Mi, and Dong Yu. Siam: Self-improving
 711 code-assisted mathematical reasoning of large language models. *arXiv preprint arXiv:2408.15565*,
 712 2024.

713 Qiying Yu, Zheng Zhang, Ruofei Zhu, Yufeng Yuan, Xiaochen Zuo, Yu Yue, Weinan Dai, Tiantian
 714 Fan, Gaohong Liu, Lingjun Liu, et al. Dapo: An open-source llm reinforcement learning system at
 715 scale. *arXiv preprint arXiv:2503.14476*, 2025.

716 Yang Yu. Pass@ k metric for rlvr: A diagnostic tool of exploration, but not an objective. *arXiv*
 717 *preprint arXiv:2511.16231*, 2025.

718 Lifan Yuan, Wendi Li, Huayu Chen, Ganqu Cui, Ning Ding, Kaiyan Zhang, Bowen Zhou, Zhiyuan
 719 Liu, and Hao Peng. Free process rewards without process labels. *arXiv preprint arXiv:2412.01981*,
 720 2024.

721 Yang Yue, Zhiqi Chen, Rui Lu, Andrew Zhao, Zhaokai Wang, Shiji Song, and Gao Huang. Does
 722 reinforcement learning really incentivize reasoning capacity in llms beyond the base model? *arXiv*
 723 *preprint arXiv:2504.13837*, 2025.

724 Eric Zelikman, Yuhuai Wu, Jesse Mu, and Noah Goodman. Star: Bootstrapping reasoning with
 725 reasoning. *Advances in Neural Information Processing Systems*, 35:15476–15488, 2022.

726 Thomas Zeng, Shuibai Zhang, Shutong Wu, Christian Classen, Daewon Chae, Ethan Ewer, Minjae
 727 Lee, Heejoo Kim, Wonjun Kang, Jackson Kunde, et al. Versaprm: Multi-domain process reward
 728 model via synthetic reasoning data. *arXiv preprint arXiv:2502.06737*, 2025a.

729 Weihao Zeng, Yuzhen Huang, Qian Liu, Wei Liu, Keqing He, Zejun Ma, and Junxian He. Simplerl-
 730 zoo: Investigating and taming zero reinforcement learning for open base models in the wild. *arXiv*
 731 *preprint arXiv:2503.18892*, 2025b.

732 Yongcheng Zeng, Guoqing Liu, Weiyu Ma, Ning Yang, Haifeng Zhang, and Jun Wang. Token-level
 733 direct preference optimization. In *Forty-first International Conference on Machine Learning*.

734 Danyang Zhang, Situo Zhang, Ziyue Yang, Zichen Zhu, Zihan Zhao, Ruisheng Cao, Lu Chen, and
 735 Kai Yu. Program: Build better gui agents with progress rewards. *arXiv preprint arXiv:2505.18121*,
 736 2025.

737 Han Zhong, Guhao Feng, Wei Xiong, Xinle Cheng, Li Zhao, Di He, Jiang Bian, and Liwei Wang.
 738 Dpo meets ppo: Reinforced token optimization for rlhf. In *ICML 2024 Workshop on Models of*
 739 *Human Feedback for AI Alignment*.

740 Mingkang Zhu, Xi Chen, Zhongdao Wang, Bei Yu, Hengshuang Zhao, and Jiaya Jia. Tgdpo:
 741 Harnessing token-level reward guidance for enhancing direct preference optimization. In *Forty-
 742 second International Conference on Machine Learning*.

743

744

745

746

747

748

749

750

751

752

753

754

755

756 **A APPENDIX**
757758 **A.1 LIMITATIONS AND FUTURE WORK**
759760 While our study demonstrates that Progressively Ascending Confidence Reward (PACR) provides a
761 powerful inductive bias for mathematical and logical reasoning, we acknowledge that our current
762 evaluation is primarily confined to natural language Chain-of-Thought (CoT).763 **Extension to Multimodal Reasoning.** A direct extension of this work is to investigate the efficacy
764 of the PACR framework in multimodal domains. Visual math problems, for instance, require Vision
765 Language Models (VLMs) to ground reasoning in visual evidence. We hypothesize that the principle
766 of uncertainty reduction applies equally to visual grounding, making this a promising direction for
767 future research.
768769 **Extension to Code-Aided Reasoning.** Furthermore, we note the growing paradigm of **code-aided**
770 **reasoning**, where models utilize external tools or generate Python code to verify intermediate logic
771 rather than relying solely on natural language (Chen et al., 2022; Gao et al., 2023; Gou et al., 2023;
772 Yu et al., 2024; Yang et al., 2025b). In this domain, applying the standard newline-based segmentation
773 would be suboptimal due to the syntactic density of code. However, the PACR framework is designed
774 to be modular with respect to step granularity. For code-aided tasks, we propose redefining the
775 “reasoning step” as the execution of a functional code block (e.g., the entire content within code
776 delimiters). We posit that the execution of such a block and the retrieval of its output constitutes
777 a single, rigorous event of *uncertainty reduction*. Extending the dense confidence signal to these
778 executable environments represents a high-value direction for future work.
779780 **A.2 BROADER IMPACT**781 This work introduces a new inductive bias designed to improve the reasoning capabilities of Large
782 Language Models. By leveraging the model’s intrinsic confidence dynamics, our method provides
783 fine-grained, step-level supervision without the significant overhead of training separate reward
784 models or requiring manual data annotation. By eliminating the need for external process-reward
785 models or human-annotated datasets, this research significantly lowers the computational and financial
786 barriers to entry for training sophisticated reasoning agents.
787788 **A.3 THE USE OF LLMs**789 We used LLMs solely for light editing such as correcting grammatical errors and polishing some
790 words. They did not contribute to research ideation, experiments, analysis, or substantive writing. We
791 have reviewed all AI-assisted edits and take full responsibility for the final content of this paper.
792793 **A.4 ETHIC STATEMENT**795 This research adheres to the highest standards of academic integrity. All existing work is appropriately
796 cited, and this paper does not violate the use of others’ work without reference. The experiments
797 conducted do not introduce new datasets or utilize any sensitive data.
798799 **B REASONING SEGMENTATION STRATEGY**
800801 A critical prerequisite for any process-based reward framework is the decomposition of the reasoning
802 trajectory $\tau^{(i)}$ into a discrete sequence of steps $\{h_k^{(i)}\}_{k=1}^{K_i}$. The definition of a “step” determines the
803 granularity of credit assignment and directly impacts the stability of the reward signal.
804805 Existing literature in process supervision typically adopts one of three segmentation paradigms:
806807

- 808 **Format-Constrained Segmentation (via SFT):** Some methods rely on Supervised Fine-
809 Tuning (SFT) to enforce rigid output structures, training the model to generate explicit tokens
such as “`<step>`” or “`Step k:`”. While this trivializes the parsing process, it introduces a
dependency on high-quality, human-annotated process data to bootstrap the format. In this

810 work, we follow the **DeepSeek-R1-Zero** paradigm (Guo et al., 2025), aiming to incentivize
 811 reasoning capabilities directly from the base model via RLVR without relying on extensive
 812 supervised cold-start data. Consequently, strategies requiring pre-learned delimiters are
 813 incompatible with our training objective.

814 • **Dynamic Entropy-Based Segmentation:** Recent works have explored leveraging intrinsic
 815 uncertainty signals to segment reasoning. For example, Liu et al. (2025a) propose dividing
 816 steps at points of high perplexity, hypothesizing that these represent semantic decision
 817 boundaries. While theoretically elegant, these methods add computational overhead during
 818 training and can be unstable during the early phases of RL when the model’s probability
 819 distribution is shifting rapidly.

820 • **Heuristic Delimiter-Based Segmentation:** The most widely adopted approach in the
 821 process reward literature (Yang et al., 2025d; Zeng et al., 2025a; Lee et al., 2025) utilizes
 822 linguistic heuristics to identify thought boundaries. Common delimiters include newline
 823 characters (`\n`) or sentence-terminating punctuation (e.g., “.”). **We adopt this strategy in**
 824 **our work.** Beyond its computational efficiency, this method aligns with the natural syntac-
 825 tic structure of Chain-of-Thought reasoning, where newlines typically signal a transition
 826 between logical operations.

827 C TRAINING DETAILS

830 We present the details of our training configuration as follows. We use a total batch size of 128 and
 831 perform one PPO epoch per rollout. The per-device batch size is set to 4 for Qwen2.5-Math-1.5B,
 832 and 2 for both Qwen2.5-Math-7B and Qwen3-4B. During rollouts, we use a sampling temperature of
 833 1.0 and generate 8 rollouts per prompt. For optimization, we use the AdamW optimizer (Loshchilov
 834 & Hutter, 2017) with a constant learning rate of 1e-6, without warmup or scheduler. The maximum
 835 prompt and generation lengths are set to 1024 and 3000 tokens, respectively. For the KL penalty, we
 836 set the coefficient $\beta = 0$, effectively deactivating it during training. For the λ_1 , and λ_2 , we search in
 837 the range of [1, 0.99, 0.9, 0.8, 0.5] and [0.01, 0.1, 0.2, 0.5], and for the both sparse and dense setting,
 838 λ_1 and λ_2 are set to 0.9, and 0.1, respectively

839 D PROMPT USED FOR OBSERVATION

840 To analyze the coherence of the reasoning paths (Observation 2) and the correlation between the
 841 large stepwise confidence gain and the pivotal reasoning step (Observation 3) in Section 4.1, we
 842 utilize GPT-5 as an evaluator. The prompts used to evaluate the reasoning steps for these respective
 843 observations are shown in Figures 9 and 10.

844 E EXAMPLES FOR OBSERVATION 3

845 This section provides additional qualitative examples that support the central claim of Observation 3.
 846 As illustrated by the reasoning trajectories from Qwen2.5-Math-7B (Figure 11) and GPT-OSS-20B
 847 (Figure 12, 13 and 14), large positive spikes in the stepwise confidence gain C_k consistently align
 848 with pivotal problem-solving steps, such as applying a key formula or executing a critical calculation.

849 **Discussion: Confidence Saturation in Post-Pivotal Steps.** We also observe a phenomenon we
 850 term “confidence saturation.” In some trajectories, after a pivotal step yields a massive confidence
 851 gain (e.g., $C_k > +2.0$), the immediately subsequent steps often exhibit near-zero gains ($C_{k+1} \approx 0$),
 852 even when they represent valid and necessary algebraic manipulations.

853 While this might initially appear as a failure of the metric (under-rewarding valid steps), we argue that
 854 it correctly reflects the information dynamics of reasoning. Once the pivotal insight is established,
 855 the remaining uncertainty regarding the final answer drops significantly. Crucially, our advantage
 856 formulation utilizes Min-Max normalization rather than Z-score normalization (as discussed in
 857 Section 7.5). This design choice ensures that the reward signal remains strictly non-negative ($R \in$
 858 $[0, 1]$). Consequently, these valid post-pivotal steps receive a neutral reward rather than a negative
 859 penalty. This prevents the optimization process from actively discouraging necessary execution steps.

864
865
866
867868
869
870
871
872
873
874
875876
877
878
879
880
881
882
883
884

USER

You are a strict verifier. Given a question, and a proposed thinking process, assign a LOGIC score from 0-5 for how logically valid the thinking is.

Scoring rubric (integers only):

- 5 = Fully sound: steps follow logically from the question; no gaps; math/symbol use correct.
- 4 = Mostly sound: one minor gap/assumption or small imprecision; overall valid.
- 3 = Mixed: at least one non-trivial gap or unjustified step; partially correct reasoning.
- 2 = Largely flawed: major gaps, speculative leaps, or misuse of evidence; little support.
- 1 = Almost entirely illogical: mostly wrong or incoherent reasoning.
- 0 = Nonsensical/contradictory or unrelated to the question.

Rules:

- Evaluate the thinking itself, not whether the final option is correct.
- Assume minor grammar issues are irrelevant.
- Do not penalize brevity if logically sufficient.
- Refer to visible evidence briefly, but DO NOT reveal your own chain-of-thought.
- Output JSON ONLY with fields: `{"justification": "<<=40 words>", "score": <0-5>"}.`

Question: `{question}`
Proposed thinking:
`{rationale}`

Output a LOGIC score from 0-5 for how logically valid the thinking is.

885 Figure 9: **Prompt used to evaluate reasoning quality for Observation 2.**886
887
888
889
890
891
892
893
894895
896
897

USER

You are a PAIRWISE key-step judge.

Goal: Given a question, the full reasoning trajectory, and its predicted answer, decide which candidate step (i or j) more causally increases the likelihood of arriving at the given predicted answer.

VALID_IDS = `{valid_indices}`

Inputs:

- Question: `{question}`
- Full reasoning trajectory (JSON array of objects `{id, text}`): `{steps_json}`
- Predicted answer: `{predicted_answer}`
- Compare: `i = {i}, j = {j}`

Decision rules:

- Judge only by causal contribution toward the *predicted* answer within the provided steps.
- Prefer the step that adds or applies a decisive constraint, calculation, elimination, or conclusion that moves the reasoning closer to (or locks in) the predicted answer.
- Do not infer facts or use outside knowledge. Use VALID_IDS only.

Output (STRICT JSON; no extra text):
`{"winner": "i" | "j" | "TIE"}`

911 Figure 10: **Prompt used to evaluate pairwise comparison for the impactful reasoning steps in Observation 3.**912
913
914
915
916
917

918
919
920
921
922
923
924
925
926
927
928
929
930
931
932
933
934
935
936

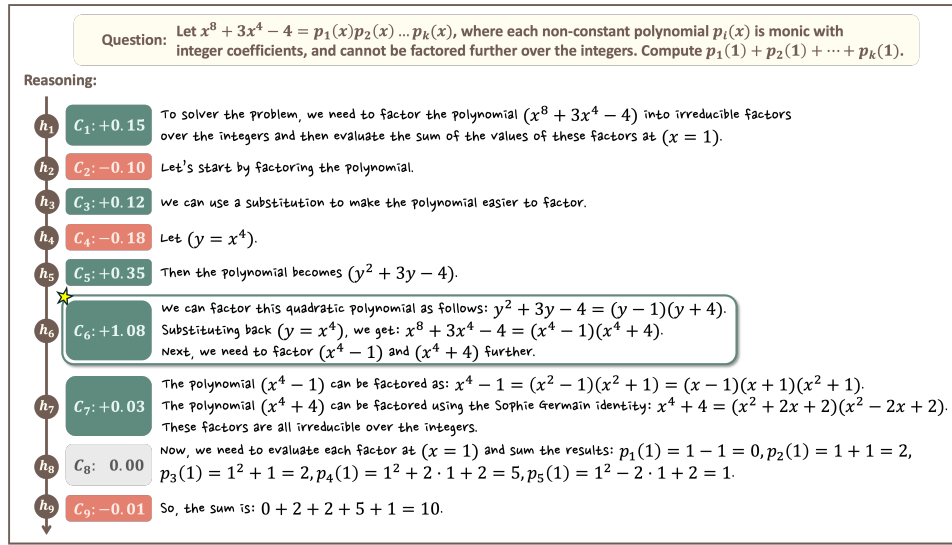


Figure 11: **Example trajectory from Qwen2.5-Math-7B for a polynomial factorization problem.** The model tackles the 8th-degree polynomial by reducing it to a quadratic form, then applying systematic factorization to break it down into irreducible integer-coefficient components. The pivotal moment occurs at step h_6 , where the model executes the core factorization. By successfully factoring the simplified quadratic expression $y^2 + 3y - 4$ and subsequently substituting x^4 back in for y , the model achieves the central algebraic decomposition of the original polynomial into two more tractable factors ($x^4 - 1$ and $x^4 + 4$). This step represents the main breakthrough required to solve the problem, and the corresponding confidence gain ($C_6 = +1.08$) indicates the model's recognition that the most significant hurdle in the factorization process has been overcome.

945
946
947
948
949
950
951
952
953
954
955
956
957
958
959
960
961
962

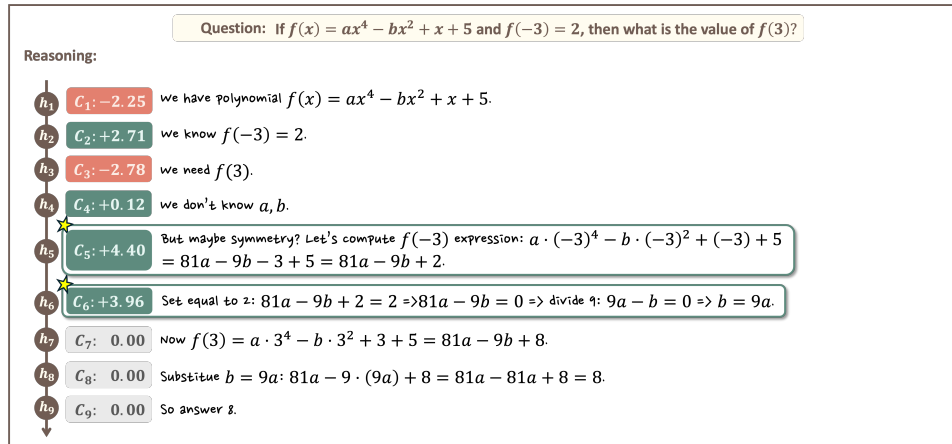


Figure 12: **Example trajectory from GPT-OSS-20B for a polynomial symmetry problem.** The problem appears ostensibly unsolvable due to the unknown coefficients a and b . The critical insight emerges across steps h_5 and h_6 , where the model leverages the inherent symmetry of the function's even-powered terms ($ax^4, -bx^2$) and utilizes the given condition $f(-3) = 2$. By evaluating the expression for $f(-3)$ and equating it to 2, the model uncovers the essential relationship between the unknown coefficients ($b = 9a$). This discovery is the pivotal moment that unlocks the entire problem, as it enables the cancellation of the unknown terms in the subsequent calculation of $f(3)$.

971

972
973
974
975
976
977
978
979
980
981
982
983
984
985
986
987
988
989

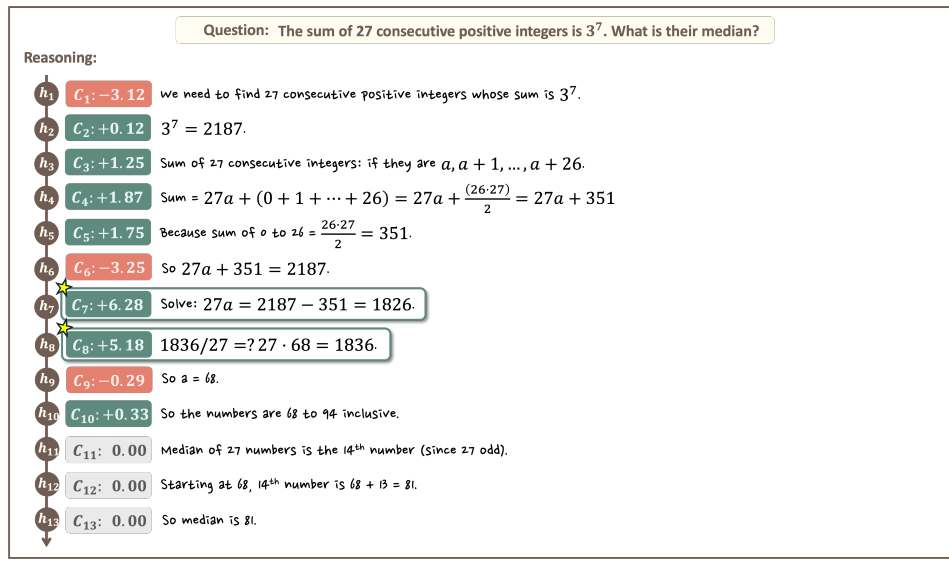


Figure 13: Example trajectory from GPT-OSS-20B for a consecutive integer median problem. The initial phase of this problem involves correctly establishing an algebraic equation for the sum of the integers: $27a + 351 = 2187$. The pivotal moment is a two-step process spanning h_7 and h_8 . In h_7 , the model transitions from algebraic formulation to the decisive computation to solve for the first integer, a , by successfully isolating the term $27a$. This is immediately followed by the critical execution in h_8 , where the actual division is performed to find the explicit value of a . Securing the value of a is the primary breakthrough, as it provides the key to determining all numbers in the sequence and thus the median.

990
991
992
993
994
995
996
997
998
999
1000
1001
1002
1003
1004
1005
1006
1007
1008
1009
1010
1011
1012
1013
1014
1015
1016
1017

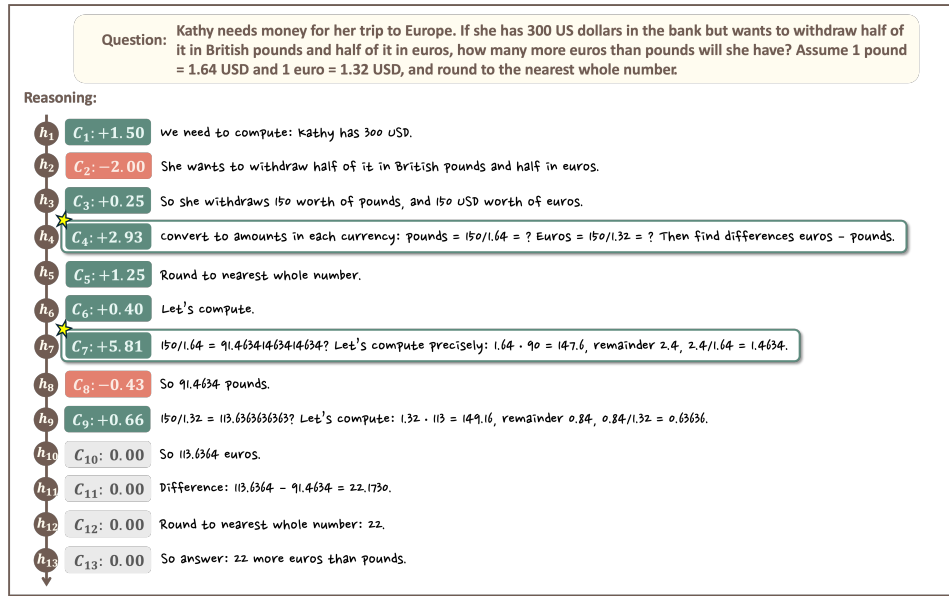


Figure 14: Example trajectory from GPT-OSS-20B for a currency exchange problem. This reasoning trajectory features two pivotal moments. First, step h_4 serves as a critical planning phase, where the model correctly formulates the computational roadmap required for the solution: two currency conversions via division, followed by a subtraction. This demonstrates a comprehensive understanding of the problem's logic. The second, more significant pivotal moment occurs at the execution phase in step h_7 , where the model accurately performs the first of the two required divisions. Successfully clearing this key computational hurdle provides the model with high confidence ($C_7 = +5.81$) that its strategy is effective and the path to the final answer is now clear.

1026 F LABEL ACQUISITION FOR STEP QUALITY ANALYSIS

1028 To empirically validate that confidence growth accurately tracks fine-grained reasoning quality
 1029 (Section 4.1), we required a set of ground truth quality labels for individual reasoning steps. We con-
 1030 structed a high-quality annotated set using a state-of-the-art Large Language Model as a programmatic
 1031 annotator.

1033 F.1 ANNOTATION SETUP

1035 We sampled a diverse set of reasoning trajectories generated by the Qwen2.5-Math-7B,
 1036 GPT-oss-20B, and Qwen3-4B models from the MATH benchmark (Hendrycks et al.) test set.
 1037 Each trajectory was first segmented into discrete steps following the delimiter-based rules described in
 1038 Section 3. Subsequently, we utilized gpt-5.1 (snapshot 2025-11-13) to classify every individual
 1039 step’s quality within these trajectories.

1040 To define the quality criteria, we adopted the taxonomy established in previous process supervision
 1041 literature Lightman et al. (2023), adapting it to capture the granularity of information gain. The model
 1042 was provided with the relevant context (Question, Final Ground Truth, Reasoning History up to the
 1043 current step) and the specific Candidate Step. The exact system instruction provided to the annotator
 1044 is as follows:

1045 **Prompt: System Instruction for Step Quality Annotation**

1046 **Role:** You are grading ONE intermediate step in a student’s solution
 1047 to a math problem.

1048 **Rate the quality of the CURRENT step using exactly these labels:**

- 1049 • **GREAT:** A strong step that a good math student might take.
 1050 It clearly moves the solution forward or is a reasonable
 1051 attempt to make mathematical progress, even if it’s not
 1052 perfectly optimal.
- 1053 • **OKAY:** Plausible but low-value. It may restate or lightly
 1054 rephrase things, check an obvious detail, or otherwise fail
 1055 to add real insight or progress, but it is not clearly wrong
 1056 or misleading.
- 1057 • **BAD:** Confidently wrong, off-topic, incoherent, or clearly
 1058 leading the solution toward a dead end; OR technically
 1059 correct but explained so poorly that a typical student could
 1060 not follow it.

1061 **Context Rule:** Always judge the current step in the context of the
 1062 problem and the previous steps.

1063 **Output Format:** Respond with STRICT JSON only, of the form:

- 1064 • rating ("Great" | "Okay" | "Bad")
- 1065 • reason ("short explanation")

1066 Do not include any extra keys or any text outside the JSON.

1067 **Input Template:**

1068 Problem: {question}
 1069 Ground-truth final answer (if available): {gt_answer}
 1070 Model’s final answer (if available): {model_final_answer}
 1071 Reasoning so far (steps 1..k, including the current step):
 1072 {steps_up_to_str}
 1073 Current step to rate (this is the LAST step above):
 1074 {current_step_text}
 1075 Now output JSON only.

1076 **Handling Error Propagation (First-Error Truncation).** Consistent with the labeling method
 1077 used in (Lightman et al., 2023), we adopt a “first-error” truncation strategy. Since language models
 1078 are autoregressive, every reasoning step is conditioned on the entire preceding history. Consequently,
 1079 once a step is labeled **BAD** (indicating a logical error or hallucination), the validity of all subsequent

1080
 1081 steps is compromised by the flawed context. To avoid the ambiguity of grading reasoning based
 1082 on false premises, we terminate annotation immediately upon encountering the first **Bad** step; all
 1083 subsequent steps in that trajectory are excluded from our analysis.
 1084

1084 F.2 VALIDATION OF LABEL QUALITY

1085
 1086 To verify the reliability of this automated annotation, we performed a rigorous inter-annotator
 1087 agreement study:
 1088

- 1089 1. **Human Inter-Annotator Agreement:** Two human experts (graduate students in mathematics/computer science) independently annotated a random subset of 100 steps. They achieved
 1090 a Cohen’s Kappa of $\kappa = 0.76$, indicating that the distinction between Great, Okay, and Bad
 1091 steps is well-defined and unambiguous to humans.
 1092
- 1093 2. **Model-Human Alignment:** We compared the primary gpt-5.1 annotations against the
 1094 human consensus on the same subset. The model achieved a Kappa score of $\kappa = 0.72$
 1095 (Table 5). This substantial alignment confirms that the model effectively acts as a reliable
 1096 proxy for human judgment, correctly adhering to the strict definitions provided in the
 1097 prompt.
 1098

1099
 1100 **Table 5: Inter-Annotator Agreement Scores.** The substantial agreement ($\kappa > 0.7$) validates that the
 1101 labels are reliable proxies for reasoning quality.

1102 Comparison Pair	1103 Metric Interpretation	1104 Cohen’s κ
1104 Human Expert 1 vs. Expert 2	1105 Task Definition Quality	0.76
1105 GPT-5.1 vs. Human Consensus	Proxy Reliability	0.72

1107 G THEORETICAL MOTIVATION FOR GROUND-TRUTH CONFIDENCE GROWTH 1108 AS A PROCESS REWARD

1109
 1110 Building on our empirical findings, we provide the theoretical motivation for using confidence growth
 1111 as a process reward. We demonstrate that maximizing this reward mathematically aligns the model’s
 1112 reasoning process with a superior “oracle” distribution conditioned on the correct answer.
 1113

1114
 1115 **The Oracle Policy: Conditioning on the correct answer as a superior policy** We define the
 1116 *oracle policy*, π_{oracle} , as the model’s generative process when conditioned on the ground-truth answer
 1117 Y_{gt} :

$$1119 \pi_{\text{oracle}}(h_k) \triangleq \pi_{\theta}(h_k \mid q, Y_{\text{gt}}, H_{<k})$$

1120
 1121 A critical premise is that π_{oracle} represents a “better” policy than the training policy π_{θ} (which
 1122 generates steps without access to the answer). Framing the policy conditioned on the correct answer
 1123 as a superior objective aligns with recent works (Zelikman et al., 2022; Wang et al., 2025), which
 1124 uses a ground-truth conditioned policy to sample good reasoning steps.

1125
 1126 **Confidence Gain as Implicit Imitation** We now show how our proposed reward, confidence gain
 1127 (C_k), leverages this oracle distribution. Recall the definition of C_k from Eq. 6:

$$1128 C_k = \log \pi_{\theta}(Y_{\text{gt}} \mid q, H_{\leq k}) - \log \pi_{\theta}(Y_{\text{gt}} \mid q, H_{<k})$$

1129
 1130 Applying Bayes’ theorem to the first term, $\pi_{\theta}(Y_{\text{gt}} \mid q, h_k, H_{<k})$, allows us to express C_k as the
 1131 log-likelihood ratio between the oracle and the standard policy:

$$1132 C_k = \log \frac{\pi_{\theta}(h_k \mid q, Y_{\text{gt}}, H_{<k}) \cdot \pi_{\theta}(Y_{\text{gt}} \mid q, H_{<k})}{\pi_{\theta}(h_k \mid q, H_{<k}) \cdot \pi_{\theta}(Y_{\text{gt}} \mid q, H_{<k})} = \log \frac{\pi_{\text{oracle}}(h_k)}{\pi_{\theta}(h_k)} \quad (14)$$

1134 During training, the model generates steps h_k according to its current policy π_θ and aims to maximize
 1135 the expected reward $\mathbb{E}[C_k]$. By substituting Eq. 14 into the objective function $J(\theta)$, we obtain:
 1136

$$\begin{aligned} J(\theta) &= \mathbb{E}_{h_k \sim \pi_\theta}[C_k] \\ &= \mathbb{E}_{h_k \sim \pi_\theta} \left[\log \frac{\pi_{\text{oracle}}(h_k)}{\pi_\theta(h_k)} \right] \\ &= -D_{KL}(\pi_\theta \parallel \pi_{\text{oracle}}). \end{aligned}$$

1142 This derivation demonstrates that maximizing the confidence gain is equivalent to minimizing the KL
 1143 divergence between the current policy π_θ and the oracle policy.
 1144

H STANDARD DEVIATION FOR EXPERIMENTS

1148 **Table 6: Standard Deviation across 3 random seeds.** We report the standard deviation of pass@1
 1149 accuracy using temperature $T = 0.0$ across six benchmarks. Lower values indicate more stable
 1150 performance. Baseline Dr.GRPO shows higher variance due to training instability, whereas PACR
 1151 methods demonstrate consistently lower variance.

Base model + Method	AIME25	AIME24	AMC	MATH500	Minerva	OlympiadBench	Average
R1-distill-Qwen-1.5B (Gen. length 8k)	-	-	-	-	-	-	-
R1-distill-Qwen-1.5B + Dr.GRPO †	2.1	1.8	2.5	1.2	1.5	1.9	1.8
R1-distill-Qwen-1.5B + Sparse-PACR	0.8	0.6	1.1	0.5	0.7	0.9	0.8
R1-distill-Qwen-1.5B + Dense-PACR	0.5	0.8	0.9	0.6	0.8	0.7	0.7
Qwen2.5-Math-1.5B	-	-	-	-	-	-	-
R1-Distill-Qwen-1.5B (Gen. length 3k)	-	-	-	-	-	-	-
Qwen2.5-Math-1.5B-Instruct	-	-	-	-	-	-	-
Qwen2.5-Math-1.5B + Dr.GRPO †	1.8	2.1	2.4	1.1	1.6	1.7	1.8
Qwen2.5-Math-1.5B + Sparse-PACR	0.8	0.9	1.0	0.6	0.8	0.7	0.8
Qwen2.5-Math-1.5B + Dense-PACR	0.6	0.7	0.8	0.5	0.6	0.8	0.7
Qwen2.5-Math-7B	-	-	-	-	-	-	-
SimpleRL-Zero-7B	-	-	-	-	-	-	-
PRIME-Zero-7B	-	-	-	-	-	-	-
OpenReasoner-Zero- 7B @ 3k	-	-	-	-	-	-	-
R1-Distill-Qwen-7B @ 3k	-	-	-	-	-	-	-
Qwen2.5-Math-7B-Instruct	-	-	-	-	-	-	-
Qwen2.5-Math-7B + Dr.GRPO †	2.0	2.5	2.2	1.4	1.8	2.1	2.0
Qwen2.5-Math-7B + Sparse-PACR	0.9	0.8	1.2	0.6	0.9	0.8	0.9
Qwen2.5-Math-7B + Dense-PACR	0.7	0.8	1.0	0.5	0.8	0.9	0.8
Qwen3-4B	-	-	-	-	-	-	-
Qwen3-4B + Dr.GRPO †	2.5	2.8	2.4	1.2	1.9	2.3	2.2
Qwen3-4B + Sparse-PACR	1.1	1.2	1.4	0.7	1.0	1.3	1.1
Qwen3-4B + Dense-PACR	0.9	0.8	1.1	0.6	0.9	1.0	0.9

1169
 1170
 1171
 1172
 1173
 1174
 1175
 1176
 1177
 1178
 1179
 1180
 1181
 1182
 1183
 1184
 1185
 1186
 1187

1188 Table 7: **Comparison with Chunk-level PACR Experiment.** The green colored numbers in the
 1189 **Average** column indicate the absolute performance improvement over the Dr.GRPO baseline.

Base model + Method	AIME25	AIME24	AMC	MATH500	Minerva	OlympiadBench	Average
R1-Distill-Qwen-1.5B (Gen. length 8k)	13.3	10.0	40.9	54.6	9.2	24.1	25.4
+ Dr.GRPO	16.7	20.0	50.6	75.2	24.3	34.4	36.8
+ Dense-PACR	20.0	20.0	56.6	78.0	26.5	38.8	40.0 <small>+3.2</small>
+ Dense-PACR with chunk 2	13.3	20.0	56.6	80.8	26.1	36.4	39.7 <small>+2.9</small>
+ Dense-PACR with chunk 4	20.0	16.7	52.8	78.6	26.8	37.4	38.7 <small>+1.9</small>

I CHUNK-LEVEL PACR EXPERIMENT

As discussed in Section 7.5, a natural concern with PACR is the computational overhead incurred by calculating C_k at every reasoning step, which requires additional forward passes during the rollout phase. To mitigate this, we investigated a Chunk-Level PACR strategy, where adjacent reasoning steps are aggregated into larger chunks, and the reward is computed only at the end of each chunk (i.e., every k steps). This linearly reduces the number of required forward passes by a factor of k .

Table 7 presents the results of this ablation on the R1-Distill-Qwen-1.5B model. We observe a clear trade-off between signal density and computational efficiency. Specifically, aggregating every two steps ($k = 2$) results in an average accuracy of 39.7%. This performance is **effectively on-par** with the fully dense baseline (Dense-PACR, 40.0%), showing only a marginal decline while halving the reward computation cost. Increasing the chunk size further to $k = 4$ leads to a slightly larger drop to 38.7%, likely due to the dilution of the training signal over longer intervals. However, critically, this performance remains significantly higher than the standard Dr.GRPO baseline (36.8%). This indicates that PACR **retains its efficacy** even with coarser step granularity, offering a practical trade-off between computational cost and signal density.